Int. J. Electron. Commun. (AEÜ) 178 (2024) 155302

Contents lists available at ScienceDirect

Int. J. Electron. Commun. (AEÜ)

journal homepage: www.elsevier.com/locate/aeue

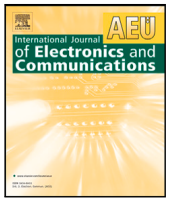

Regular paper

Performance enhancement of Vivaldi-shaped planar UWB antenna using a single-layer FSS reflector

Saad Hassan Kiani [a,*], Umair Rafique [b], Hüseyin Şerif SAVCI [c], Hatem Rmili [a,*], Naser Ojaroudi Parchin [d], Abeer D. Algarni [e], Hela Elmannai [e]

[a] Electrical and Computer Engineering Department, Faculty of Engineering, King Abdulaziz University, Jeddah, Kingdom of Saudi Arabia
[b] Center for Wireless Communications, Faculty of Information Technology and Electrical Engineering, University of Oulu, 90570 Oulu, Finland
[c] Electrical and Electronics Engineering Department, Faculty of Engineering and Natural Sciences, Istanbul Medipol University, 34810 Istanbul, Turkey
[d] School of Computing, Engineering and the Built Environment, Edinburgh Napier University, EH10 5DT Edinburgh, UK
[e] Department of Information Technology, College of Computer and Information Sciences, Princess Nourah bint Abdulrahman University, P.O. Box 84428, Riyadh 11671, Kingdom of Saudi Arabia

ARTICLE INFO

Keywords:
Planar antenna
Vivaldi-shaped patch
FSS
Radiation performance

ABSTRACT

This work proposes the design of a frequency-selective surface (FSS)-based planar monopole antenna for ultra-wideband (UWB) communication applications. The UWB response is observed by integrating a Vivaldi-shaped slot and by introducing a stepped-like pattern on the bottom edges of the radiating patch, while the back side is composed of a partial ground plane. This configuration results in a broad impedance bandwidth spanning from 3.11 to 20 GHz. For radiation performance enhancement of the proposed antenna, a single-layer UWB FSS reflector is placed beneath the antenna element at an optimized distance. The proposed FSS reflector employs a 3 × 3 array of fractal structure with a unit cell size of 12.25 × 12.25 mm^2. The designed FSS reflector exhibits a linear phase response over a frequency range of 3.28 to 14 GHz, with a stop-band transmission coefficient less than -10 dB. The incorporation of the FSS reflector results in an increased gain, elevating it from 1 to 4 dBi at low-band frequencies, while at mid-band frequencies, the gain is increased from 1 to 6 dBi. The structural configuration of the proposed antenna yields directional far-field patterns, making it well-suited for UWB radar applications.

1. Introduction

In wireless communication systems, the role of ultra-wideband (UWB) antennas is paramount, as they facilitate the efficient transmission and reception of radio signals across a broad frequency spectrum. One of the key advantages of UWB antennas is that they deliver data at exceptionally high speeds over short distances while maintaining minimal power consumption [1], making them ideal for applications such as indoor positioning, asset tracking, and rapid wireless connectivity [2]. Moreover, UWB antennas offer superior accuracy in location tracking, enhanced signal penetration through obstacles like walls and floors, and reduced susceptibility to interference from neighboring wireless devices. Consequently, the integration of UWB antennas into wireless communication systems not only improves performance but also ensures greater reliability, positioning them as a preferred choice over conventional antennas for a wide range of applications [3,4].

For UWB communication systems, it is required that the antenna element be small in size so that it can fit directly on the printed circuit board (PCB). This requirement can be fulfilled by adopting a planar antenna configurations such as planar monopoles [5], slot antennas [6], etc. The problems associated with these kinds of antennas are low gain and radiation efficiency. In addition, planar UWB antennas suffer due to high back radiation, which limits their use in applications where directive radiation properties are required. To mitigate these effects, one of the techniques is to utilize frequency-selective surface (FSS) reflectors behind the radiating element. FSS operates on the principle of selectively filtering electromagnetic (EM) waves based on their frequency, leveraging the arrangement of periodic elements on a substrate [7,8]. In the context of UWB antennas, FSS serves as a crucial component for achieving enhanced performance. The details about some of the previously presented FSS-integrated UWB antenna designs are provided in the next paragraph.

In [9], an enhanced gain trapezoidal-shaped planar antenna was designed for UWB applications. The gain of the antenna was enhanced

* Corresponding authors.
E-mail addresses: iam.kiani91@gmail.com (S.H. Kiani), hmrmili@kau.edu.sa (H. Rmili).

https://doi.org/10.1016/j.aeue.2024.155302
Received 20 December 2023; Accepted 18 April 2024
Available online 27 April 2024

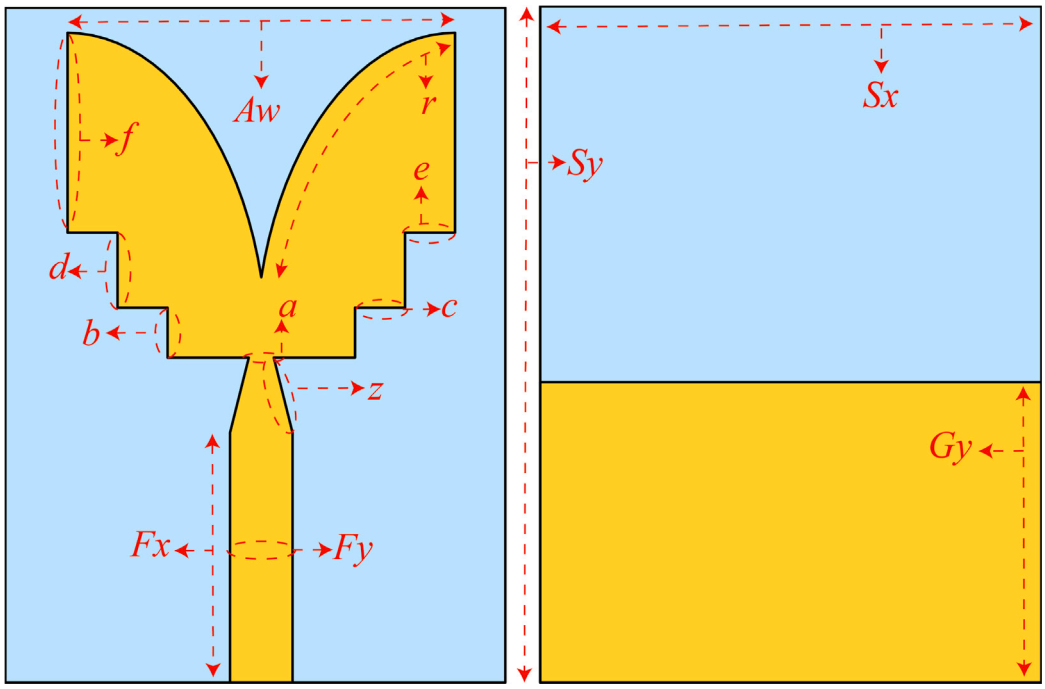

Fig. 1. Proposed UWB antenna (a) front-side (b) back-side. The dimensions of the antenna (in mm) are as: $S_x = 20$, $S_y = 27$, $G_y = 12$, $F_x = 2.5$, $A_w = 15.5$, $F_y = 13$, $a = 1$, $b = 2$, $c = 2$, $d = 3$, $e = 2$, $f = 8$, $r = 12.47$, $z = 3$.

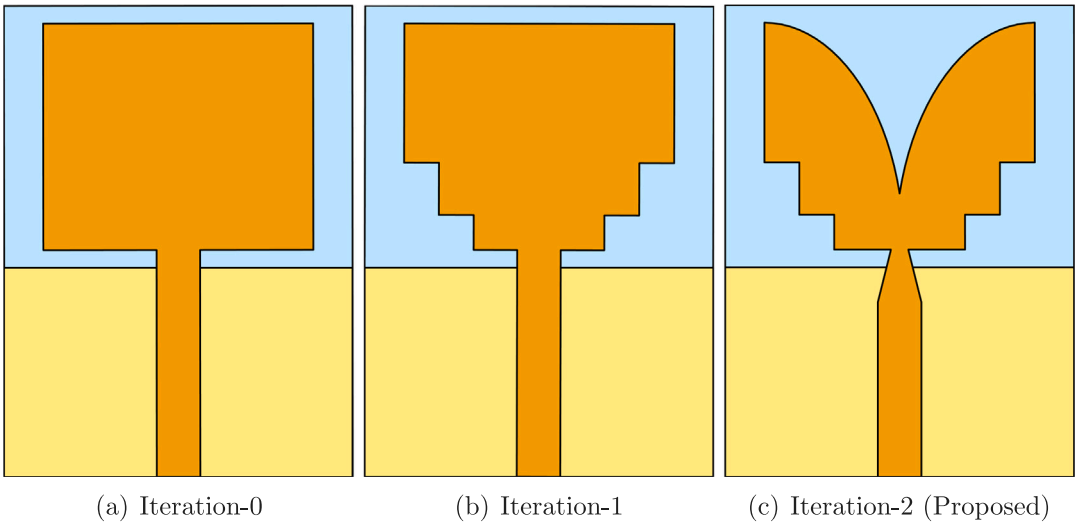

Fig. 2. Design evolution of the proposed UWB antenna. Dark orange top metal face, light orange bottom metal face (ground), and light blue dielectric substrate. (For interpretation of the references to color in this figure legend, the reader is referred to the web version of this article.)

by placing a 6 × 6 dual-layer array of modified loop structure (MLS)-based FSS. The utilization of the MLS FSS structure offered a peak gain of 9 dBi and an impedance bandwidth of 8 GHz (3–12 GHz). In [10], an umbrella-shaped co-planar waveguide (CPW)-fed monopole antenna was presented with a 4 × 4 array of dual-layer FSS structure. The top side of the FSS structure consists of a slotted square ring resonator (SRR), while the bottom side consists of a combination of square-loop and Jerusalem cross. With the help of a dual-layer FSS reflector, the authors achieved a gain enhancement of about 2–4 dB in the operating bandwidth. In [11], a dual-band planar antenna operating at 2.4 and 5.8 GHz frequency bands was presented. The gain at both frequency bands was enhanced by using a simple double-square-loop FSS element. For 2.4 GHz, the antenna exhibits directional radiation characteristics, but for the 5.8 GHz frequency band, distorted radiation characteristics are observed. The authors in [12] designed an array of modified square-loop FSS unit cells and placed them above the radiating element for radiation performance enhancement. The placement of FSS above the antenna offered a peak gain of 9 dBi in the UWB frequency band. In [13], a strawberry-shaped single-layer FSS-integrated UWB antenna was presented. A modified rectangular-loop FSS was used to achieve a peak gain of 9.68 dBi. In [14], a CPW-fed UWB antenna operating from 3.6 to 11.8 GHz was designed and integrated with an 8 × 8 array of square-loop and a ring-based FSS for gain enhancement. Through the presented configuration, a minimum 4 dB gain increase was achieved across the entire frequency range.

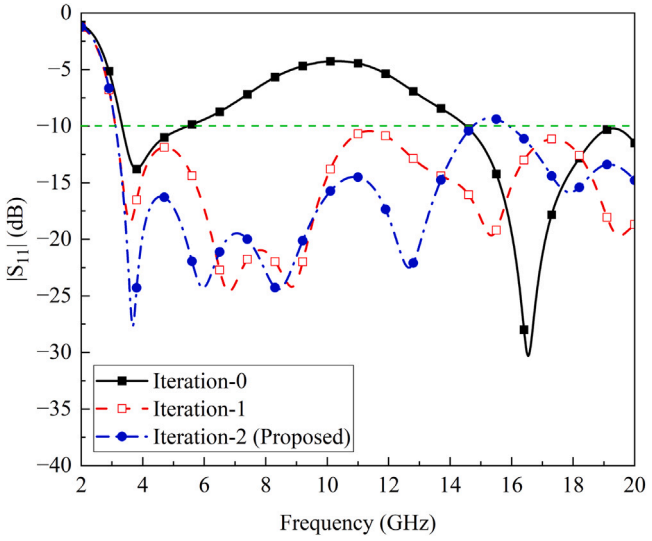

Fig. 3. Simulated $|S_{11}|$ of all the design stages shown in Fig. 2.

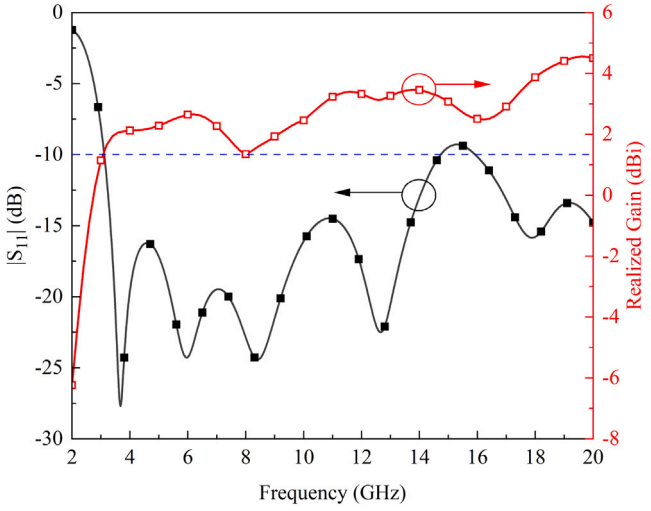

Fig. 4. Simulated $|S_{11}|$ and realized gain of the UWB antenna.

In [15], a 6 × 6 array of single-layer FSS structure was designed to increase the gain of a planar UWB antenna. A peak gain of 8.3 dBi was achieved with an 8 GHz impedance bandwidth in the UWB range. They also designed a fractal FSS structure in [16] for the gain enhancement of UWB planar antennas. The fractal FSS array operates well in the UWB frequency band, and its integration with the antenna offers a peak gain of 7.5 dBi. In [17], the authors presented a novel design of a planar antenna for UWB applications. For the performance enhancement of the antenna, a single-layer FSS structure was designed using a combination of square-loop and ring. The incorporation of the FSS layer behind the antenna increased the gain up to 10.5 dBi in the operating bandwidth, ranging from 5 to 17 GHz. In [18], the authors designed a monopole antenna that works across two frequency bands, i.e., 2.18–2.83 GHz and 4.42–5.58 GHz. The radiation performance of the dual-band monopole was enhanced with the use of a modified Jerusalem-shaped FSS reflector. The incorporation of the FSS yields notable enhancements in gain and radiation efficiency. In [19], the authors presented a novel FSS-based planar antenna design for UWB applications and achieved a peak gain of 9.5 dBi.

The UWB antenna designs discussed above offer acceptable radiation performance, but their multilayer configuration and large size may restrict their use in wireless communication devices. In addition, most of the above-presented designs are not able to provide directional radiation characteristics, which is the main focus of this work. Therefore, in this paper, a single-layer FSS reflector-based planar UWB antenna is designed to achieve high gain and directional radiation characteristics. The UWB response is obtained by designing a Vivaldi-shaped radiating element with a partial ground plane. For the enhancement of the radiation performance of the designed UWB antenna, a 3 × 3 array of single-layer fractal UWB FSS unit cells is designed and placed beneath the radiating element at an optimized distance. It is noted that the proposed UWB antenna system operates well from 3.11 to 20 GHz, offering an impedance bandwidth of 16.89 GHz. Furthermore, the integration of the FSS reflector led to an increase in gain of 4–6 dB. In the next section, a complete antenna design procedure and its results are presented.

2. Antenna design & configuration

2.1. Vivaldi-shaped planar antenna

Fig. 1 illustrates the schematic of the proposed planar antenna along with the optimized design parameters. To design the antenna, a 1.6 mm thick, low-cost FR-4 substrate with a relative permittivity (ε_r) of 4.4 is used. The radiating element consists of a Vivaldi-shaped structure backed by a partial ground plane. To achieve a UWB response, a Vivaldi-shaped slot is introduced in a radiating element, and a stepped-like pattern is designed on the bottom edges of the radiating patch.

To understand the optimization process of the proposed UWB antenna, a design evolution is presented and shown in Fig. 2. The design evolution of the proposed UWB antenna starts with the configuration of a conventional rectangular radiator backed by a partial ground plane named as iteration-0, as shown in Fig. 2(a). The reflection coefficient ($|S_{11}|$) response of the iteration-0 design is shown in Fig. 3, and it is observed that it offers a dual-band response in the band of interest. To achieve UWB response, a stepped pattern is introduced at the bottom edges of the rectangular patch (iteration-1), as shown in Fig. 2(b). The addition of a stepped pattern generates multiple resonances, which led to an impedance bandwidth of 16.89 GHz ranging from 3.11 to 20 GHz, as shown in Fig. 3. To further improve the impedance matching, a Vivaldi-shaped slot is etched from the radiating element (see Fig. 2c, iteration-2), and a modification is made in the microstrip feeding line. This modification tends to achieve improved impedance matching in the operating bandwidth, especially from 3.11 to 14 GHz, as depicted in Fig. 3.

The simulated $|S_{11}|$ response of the proposed planar antenna is shown in Fig. 4. It is noted that the designed antenna is able to resonate from 3.11 to 20 GHz (according to −10 dB bandwidth criteria), providing a fractional bandwidth (FBW) of 146.17%. Fig. 4 also depicts the simulated realized gain response of the designed antenna. The minimum gain value is observed to be 1 dBi at 3.11 GHz, while the maximum gain value is 4.55 dBi at 20 GHz.

The simulated normalized far-field radiation characteristics of the UWB antenna for both *H*- and *E*-planes are shown in Fig. 5. The patterns are plotted for five different frequency bands, i.e., 4 GHz, 8 GHz, 12 GHz, 16 GHz, and 20 GHz, which covers the entire operating range of the designed antenna. For *H*-plane, the antenna exhibits omnidirectional patterns at 4 and 8 GHz (see Figs. 5a and b). For frequencies greater than 8 GHz, the pattern becomes quasi-omnidirectional, as shown in Figs. 5(c)–5(e). This is due to the fact that the radiating area of the structure changes with frequency over UWB, which disturbs the radiation performance of the antenna. Another factor that plays a major role in deteriorating radiation patterns is the excitation of higher-order modes at higher frequencies. For the *E*-plane, a monopole-like (typical eight-shape) radiation pattern is observed for frequencies up to 16 GHz, as shown in Figs. 5(a)–5(d). For 20 GHz, a distorted pattern

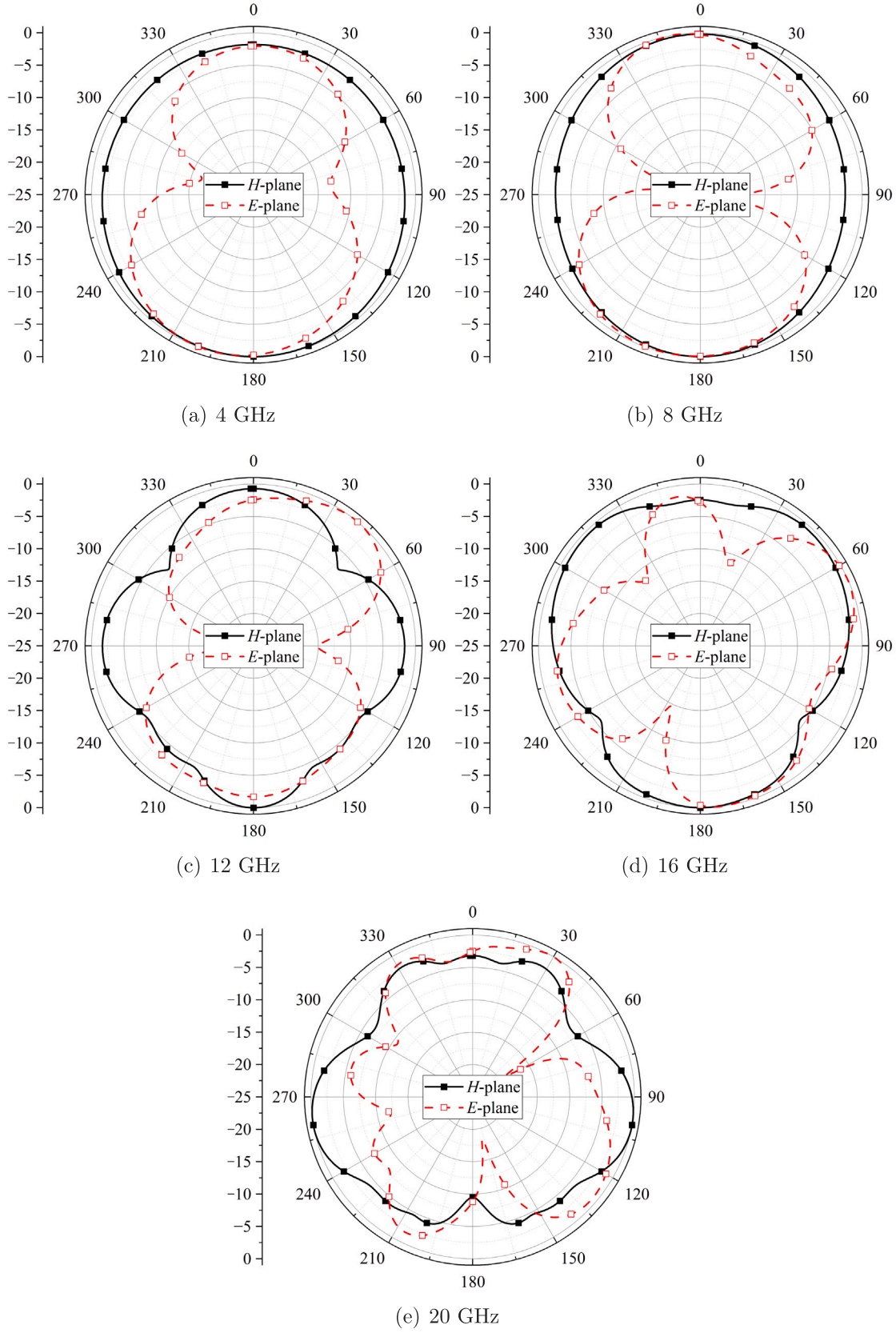

Fig. 5. Simulated normalized far-field radiation patterns of the UWB antenna.

is observed in the *E*-plane (see Fig. 5e). From the *E*-plane patterns, it is also observed that the maximum radiation is directed towards the back side, which led to the reduced antenna gain. To enhance the radiation performance of the antenna and to make it more directive, a single-layer FSS reflector is placed behind the designed antenna, whose explanation is given in the coming sub-sections.

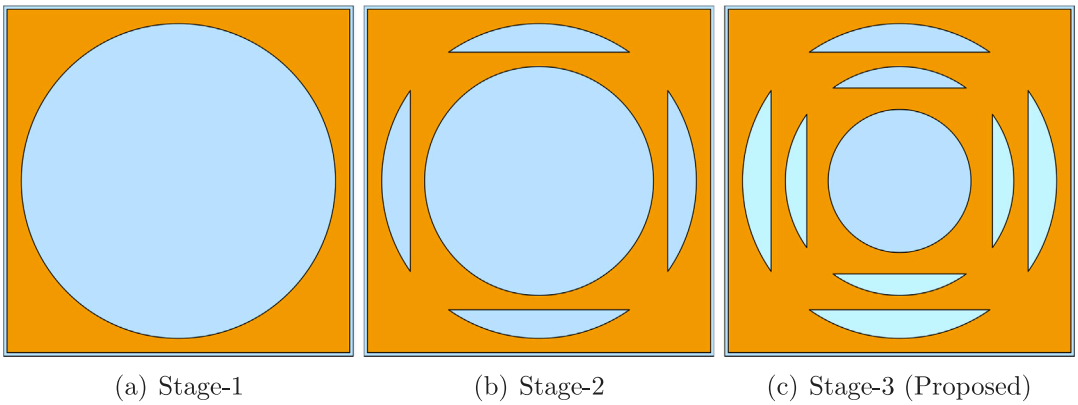

Fig. 6. Design evolution of the single-layer FSS reflector.

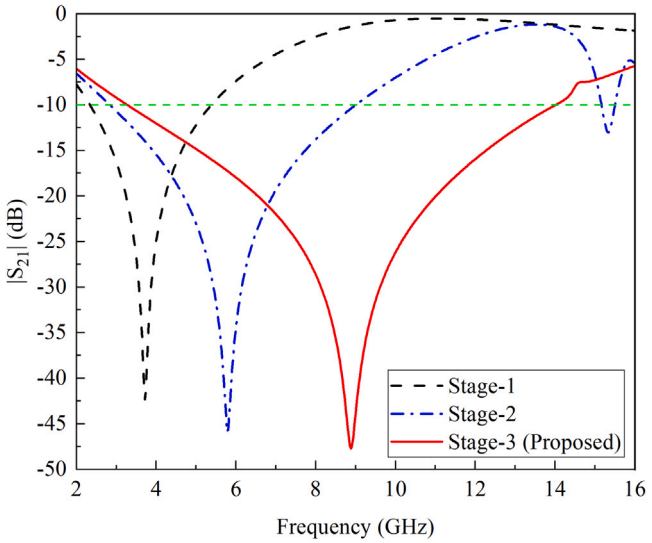

Fig. 7. Simulated $|S_{21}|$ of all the FSS design stages shown in Fig. 6.

2.2. FSS reflector design

The design of the proposed UWB FSS reflector is presented in this sub-section. The evolution process of the proposed FSS reflector is shown in Fig. 6 and the obtained transmission coefficient ($|S_{21}|$) for all the design stages is shown in Fig. 7. The design evolution is composed of three stages, namely stage-1, stage-2, and stage-3 (proposed). At first, a simple conventional circular slot is designed, as shown in Fig. 6(a) and it is observed that it is resonating around 4 GHz with a bandwidth ranging from 2.3 to 5.3 GHz (see Fig. 7). In design-2, a square patch and a circular slot are inserted (see Fig. 6b) and it was observed that the bandwidth was increased to 2.93–8.8 GHz with a central frequency of 5.82 GHz. At the proposed stage (stage-3), another square patch and circular slot are inserted, as shown in Fig. 6(c), and it is noted that the FSS reflector is operating well from 3.28 to 14 GHz, covering the desired UWB frequency band.

2.3. FSS-integrated UWB antenna

After designing the FSS reflector, the UWB antenna design, discussed in sub-section 2.1, is integrated with the FSS reflector to achieve improved radiation performance. Fig. 8 shows the design and configuration of an FSS-based planar UWB antenna. An array of FSS consists of 3 × 3 unit cells placed under the designed UWB antenna so that it can reflect the back radiation and enhance the overall radiation performance of the antenna [20]. As the FSS reflector is wideband in nature, the distance between the antenna and FSS layer is optimized during the simulation process to achieve maximum gain. The optimized value for the parameter H is noted to be 25 mm, which is equal to $\lambda_0/4$ @ 3 GHz.

The simulated $|S_{11}|$ and realized gain of the proposed UWB antenna without and with FSS are depicted in Fig. 9. It can be observed from the result of Fig. 9(a) that with the integration of FSS, the proposed UWB antenna has retained its wideband characteristics. On the other hand, when the FSS is integrated with the antenna, a significant increase is observed in the realized gain over the operating bandwidth. The maximum gain enhancement is observed at 8 GHz, where the gain increased from 1.1 to 5 dBi, as shown in Fig. 9(b).

To further evaluate the performance of an FSS-integrated UWB antenna, a parametric study is conducted by changing the distance (H) between the planar antenna and FSS reflector. The value of H is varied from 23 to 28 mm, and the performance is evaluated in terms of $|S_{11}|$ and realized gain, as shown in Fig. 10. It is observed from the results that the distance has a minor influence on the antenna performance (see Figs. 10a and 10b). The effect of FSS array configurations on the antenna's performance is shown in Fig. 11. It is observed that the gain increases as the array size increases, especially from 7 to 14 GHz (see Fig. 11a), but it provides an impedance mismatch from 3.36 to 4.5 GHz, as depicted in Fig. 11(b). Further optimizing the distance between the radiating element and the FSS reflector can reduce this mismatch at the expense of an increase in antenna system size, which is not advantageous for small devices.

3. Fabrication and measurement results

The prototype of the fabricated antenna and FSS array before and after assembly is shown in Figs. 12(a) and 12(b). To establish a separation between the antenna and FSS, a 25-mm-thick Styrofoam is carefully employed, as depicted in Fig. 12(b). The choice of Styrofoam is attributed to its minimal impact on the antenna's performance.

The simulated and measured $|S_{11}|$ of the FSS-integrated UWB antenna are depicted in Fig. 13(a). The $|S_{11}|$ were determined using a Vector Network Analyzer (VNA). The simulated and measured values offer wideband characteristics from 3.11–20 GHz. A small disagreement is observed between the results, which could arise due to connector and cable losses and fabrication tolerances. Similarly, the gain of the proposed antenna showed a peak simulated value of ≈ 6 dBi around 9 GHz, while the measured gain shows a constant behavior from 4 to 13 GHz with a value of 5 dBi, as shown in Fig. 13(b). The strong agreement between both results shows the performance stability of the proposed antenna.

Figs. 14 and 15 show the normalized simulated and measured far-field radiation characteristics of the FSS-integrated UWB antenna

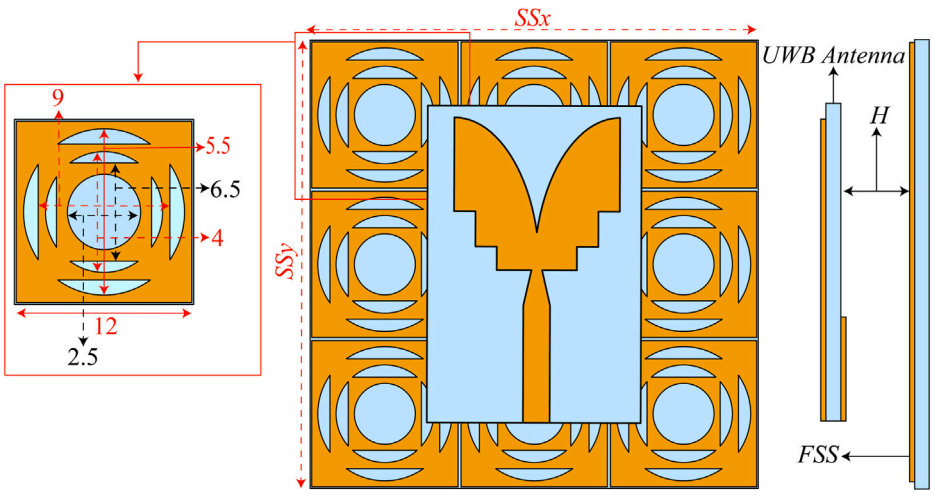

Fig. 8. Configuration of the FSS-integrated UWB antenna. The figure also shows the design values of FSS unit cell having $SS_x = SS_y = 36.75$ mm.

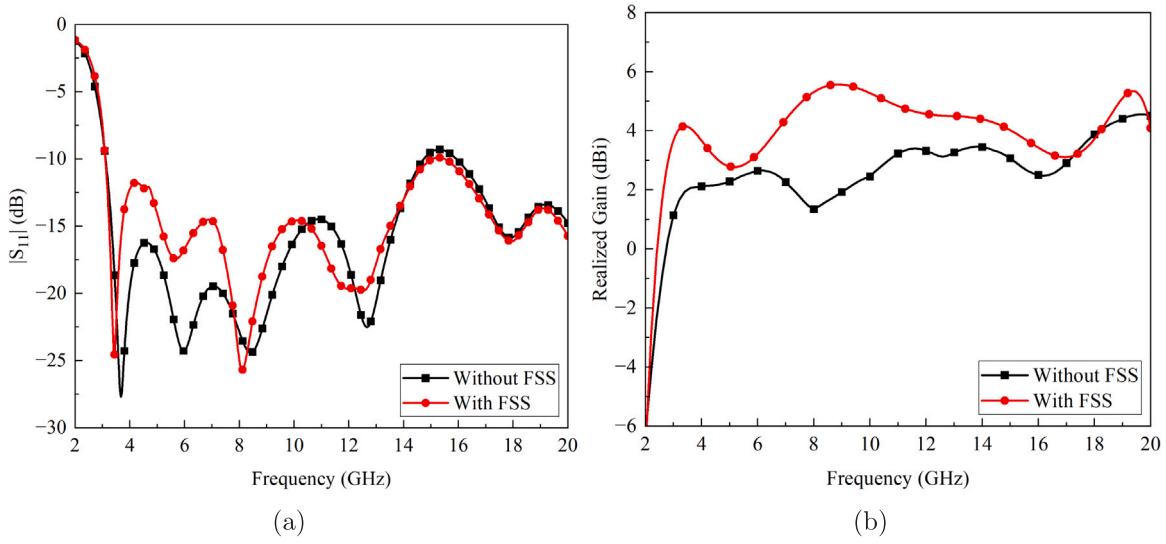

Fig. 9. Simulated (a) $|S_{11}|$ and (b) realized gain of the UWB antenna without and with FSS reflector.

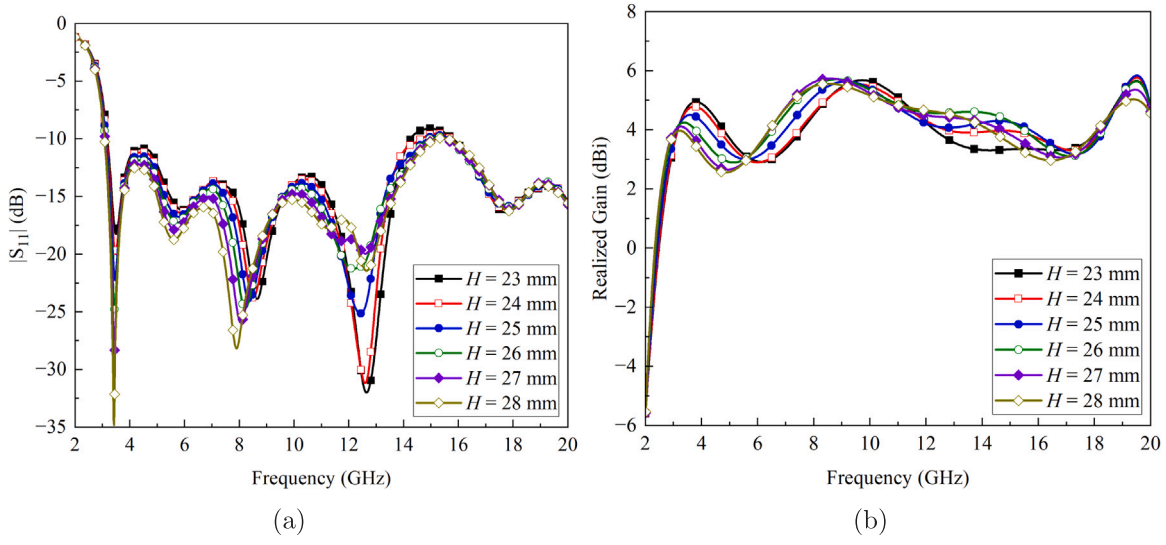

Fig. 10. Simulated (a) $|S_{11}|$ and (b) realized gain of the FSS-integrated UWB antenna for different distances.

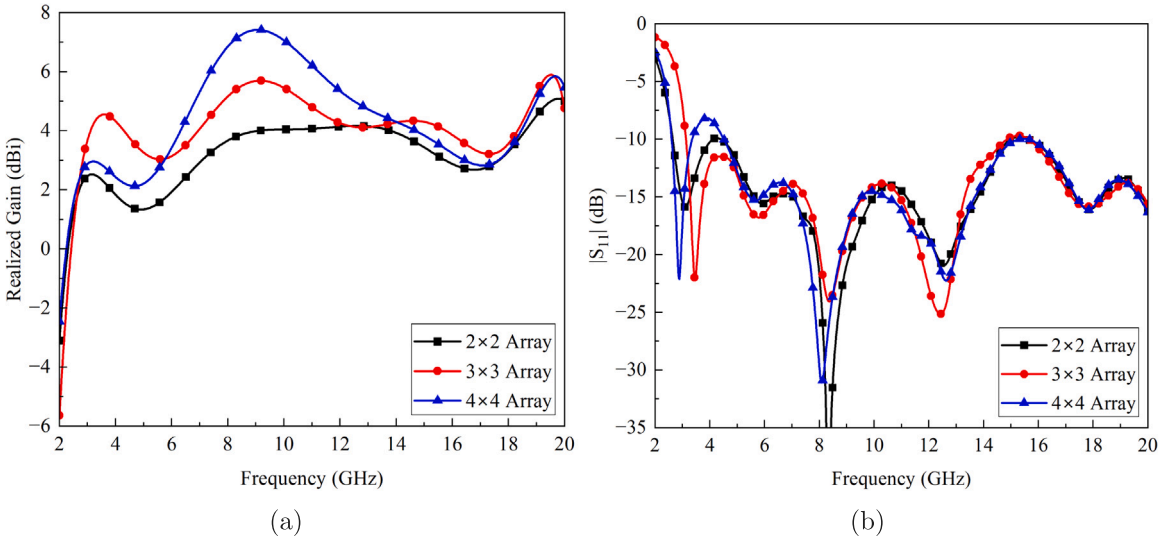

Fig. 11. Simulated (a) realized gain and (b) $|S_{11}|$ of the FSS-integrated UWB antenna for different array configurations.

Fig. 12. Fabricated prototype of FSS-integrated UWB antenna (a) before assembly (b) after assembly.

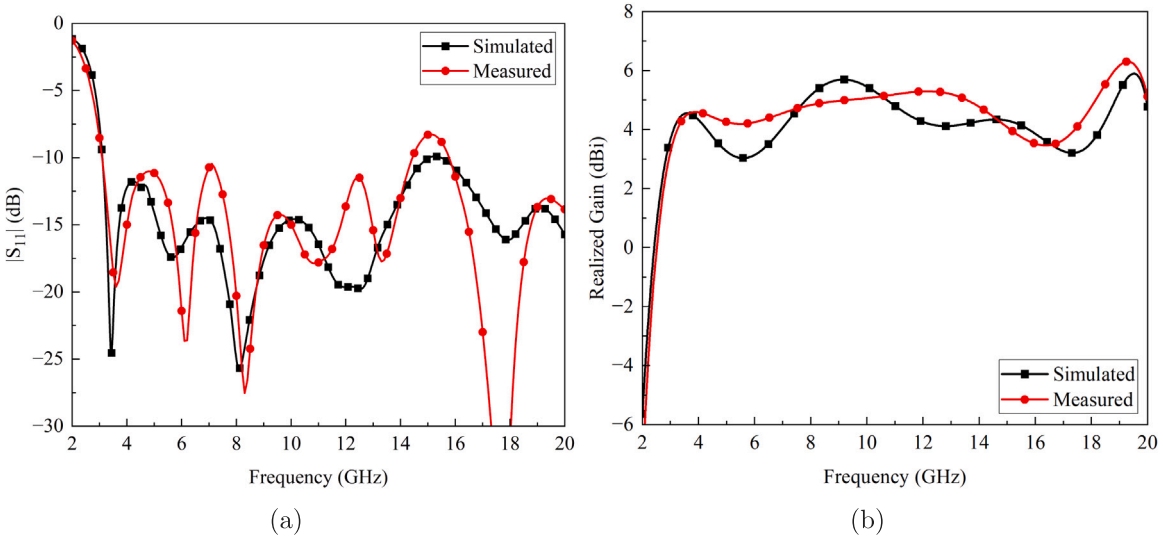

Fig. 13. Simulated and measured (a) $|S_{11}|$ and (b) realized gain of FSS-integrated UWB antenna.

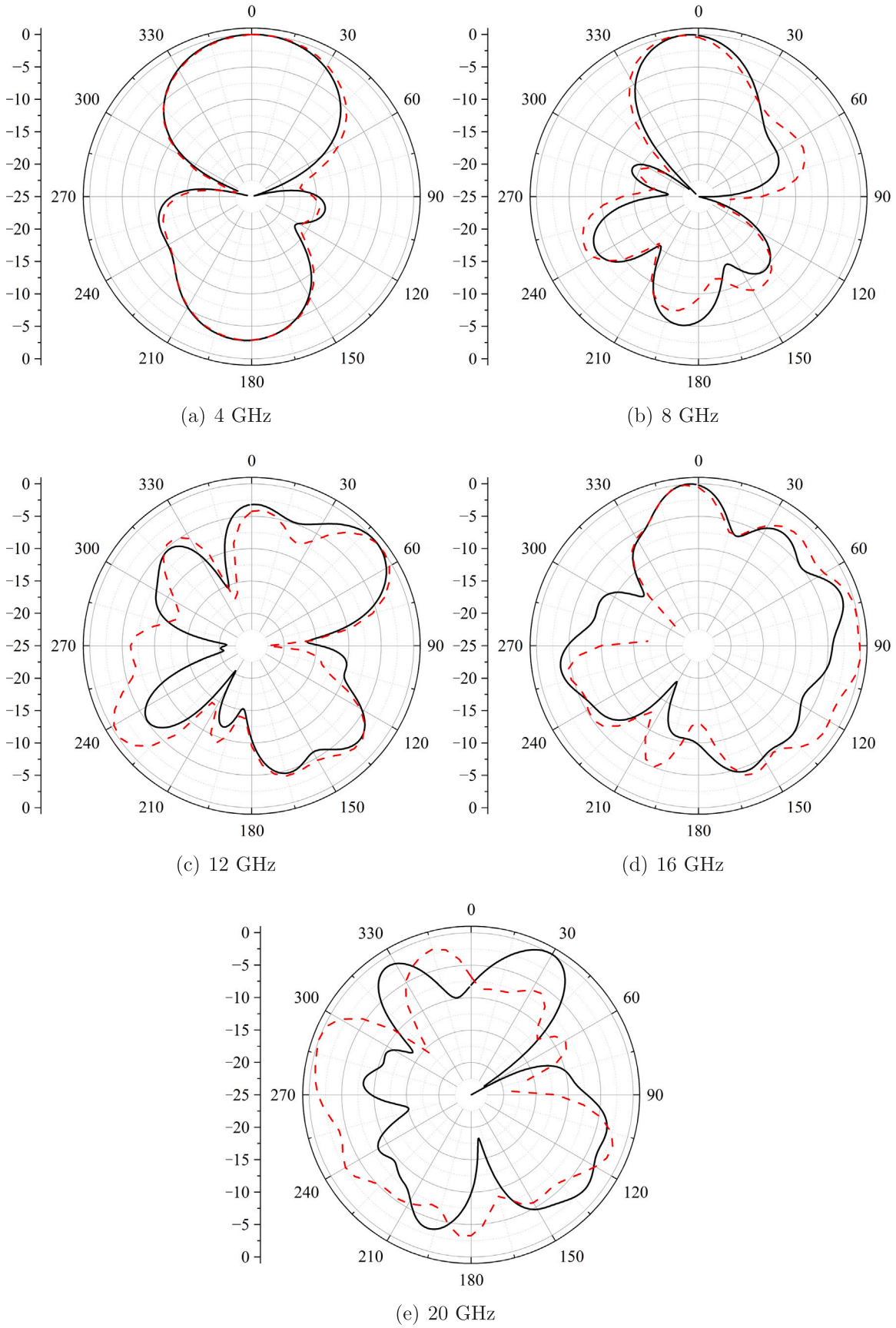

Fig. 14. Normalized *E*-plane far-field radiation characteristics of the proposed FSS-integrated UWB antenna (Solid Line: Simulated, Dash Line: Measured).

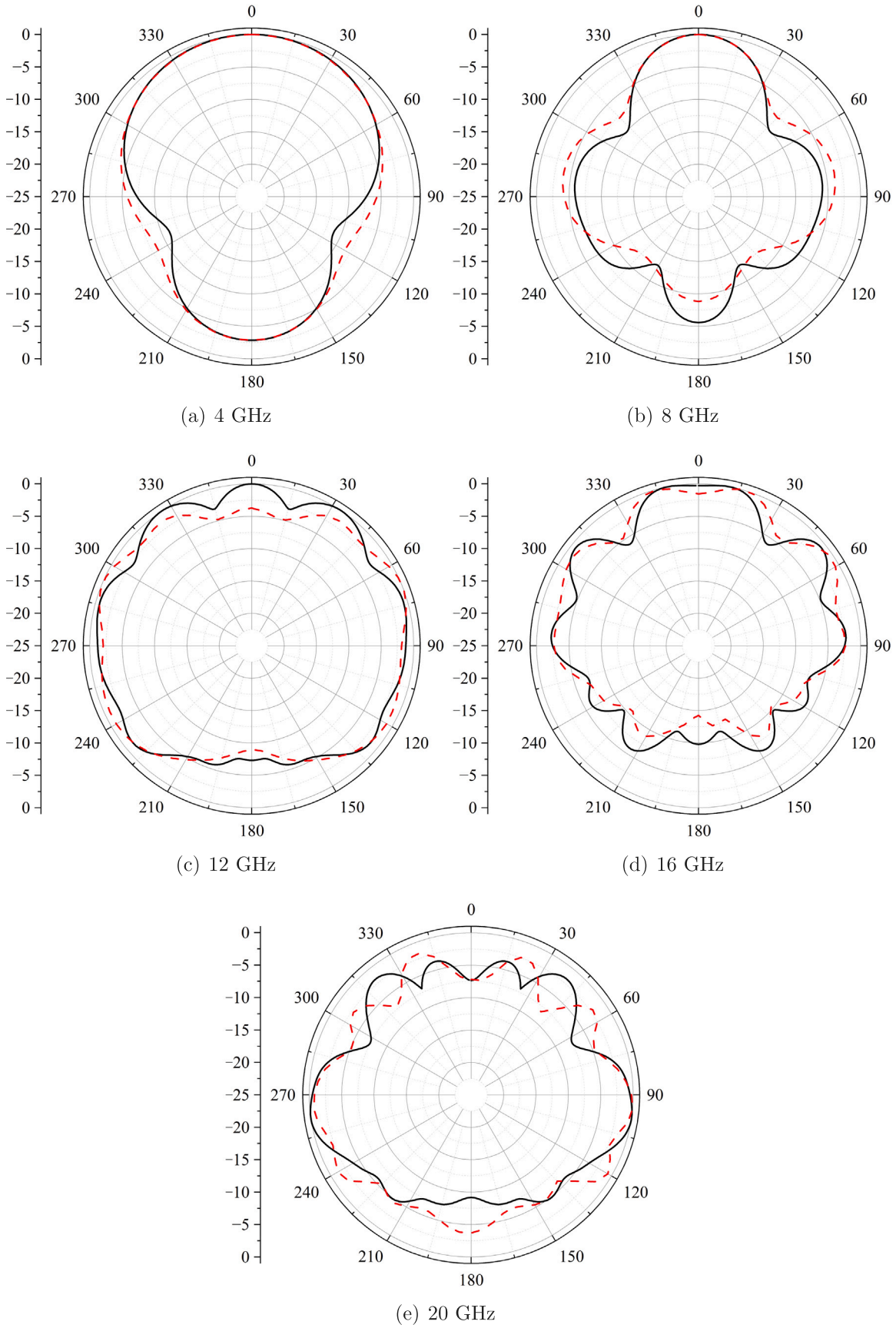

Fig. 15. Normalized H-plane far-field radiation characteristics of the proposed FSS-integrated UWB antenna (Solid Line: Simulated, Dash Line: Measured).

Table 1
Comparison of proposed FSS-integrated UWB antenna with state-of-the art literature.

Ref.	Year	Sys. Size (mm^3)	Freq. Range (GHz)	Peak gain (dBi)	Gain variation (dB)	FSS layers
[9]	2017	96 × 96 × 30	3–12	8.9	3.4	Dual
[10]	2018	44 × 44 × 25.5	3-13.5	8.5	3	Dual
[11]	2019	81 × 81 × 35.3	2.37–2.56/5.15–6.22	7.54/6.8	–	Single
[12]	2019	124 × 124 × 8	3–10	9	4	Single
[13]	2020	60 × 60 × 10	3.05–11.9	9.68	1.8	Single
[14]	2022	40 × 40 × 30	2.55–13	8.6	4.6	Single
[15]	2022	60 × 60 × 25	3–12	8.3	2.5	Single
[16]	2023	60 × 60 × 10	3.3–10.8	7.5	2.2	Single
[17]	2023	50 × 50 × 9	3–18	10.5	2.5	Single
[18]	2023	80 × 80 × 10	2.18–2.83/4.42–5.58	7.87	–	Single
[19]	2023	50 × 50 × 12	3.3–9.9	9.5	5	Single
Prop.	2024	36.75 × 36.75 × 25	3.11–20	5	2.5	Single

Sys. = System, Freq. = Frequency

for both *E*- and *H*-planes. Far-field measurements for the proposed design were conducted within a shielded anechoic chamber. In the experimental setup, the proposed antenna is placed on the receiver end and the horn antenna at the transmitter end, ensuring an ideal evaluation of the antenna's performance under controlled conditions. The patterns are plotted for five resonant frequencies, i.e., 4 GHz, 8 GHz, 12 GHz, 16 GHz, and 20 GHz. For the *E*-plane, directional radiation characteristics are observed at 4 and 8 GHz, as shown in Figs. 14(a) and 14(b). For 12, 16, and 20 GHz, distorted patterns are observed with an increase in gain (see Figs. 14c–14e). In the case of the *H*-plane, patterns are directive up to 16 GHz, as shown in Figs. 15(a)–15(d). In this case, the pattern at 20 GHz is quasi-omnidirectional (see Fig. 15e).

To highlight the performance of the proposed FSS-based UWB antenna, a comparative analysis was conducted against notable state-of-the-art counterparts (see Table 1). The performance is assessed based on the measurement results. Although the proposed design offers less gain, it exhibits a wide impedance bandwidth with stable gain compared to the designs listed in Table 1. In addition, the proposed antenna system is compact compared to the other designs.

4. Conclusions

This paper presents the design of a FSS reflector-backed Vivaldi-shaped planar monopole antenna for UWB characteristics. The designed UWB antenna exhibits an impedance bandwidth of 16.89 GHz in the frequency range of 3.11–20 GHz. To achieve directional radiation characteristics and high gain, an array of single-layer UWB FSS is designed and placed behind the proposed UWB antenna. It is observed that the FSS-based UWB antenna offers a peak measured gain of 5 dBi in the operating bandwidth. In addition, the simulated and measured results of the designed antenna are in good agreement. The presented configuration and results suggest that the designed FSS-integrated UWB antenna is suitable for applications requiring directional radiation properties, like ground penetrating radar (GPR) and near-field microwave imaging.

CRediT authorship contribution statement

Saad Hassan Kiani: Writing – review & editing, Writing – original draft, Software, Conceptualization. **Umair Rafique:** Visualization, Software, Conceptualization. **Hüseyin Şerif SAVCI:** Methodology, Formal analysis, Data curation. **Hatem Rmili:** Validation, Supervision, Resources. **Naser Ojaroudi Parchin:** Project administration, Methodology, Investigation, Funding acquisition. **Abeer D. Algarni:** Writing – review & editing, Software, Resources, Funding acquisition, Conceptualization. **Hela Elmannai:** Software, Project administration, Methodology, Investigation.

Declaration of competing interest

The authors declare that they have no known competing financial interests or personal relationships that could have appeared to influence the work reported in this paper.

Data availability

No data was used for the research described in the article.

Acknowledgments

The authors would like to thank Science and Technology Unit - King Abdulaziz University - Kingdom of Saudi Arabia - award number (UE-41-120) and Princess Nourah bint Abdulrahman University Researchers Supporting Project number (PNURSP2024R51), Princess Nourah bint Abdulrahman University, Riyadh, Saudi Arabia to provide the funding for this work.

Funding statement

Princess Nourah bint Abdulrahman University Researchers Supporting Project number (PNURSP2024R51), Princess Nourah bint Abdulrahman University, Riyadh, Saudi Arabia.

References

[1] Jan NA, Kiani SH, Sehrai DA, Anjum MR, Iqbal A, Abdullah M, et al. Design of a compact monopole antenna for UWB applications. Comput, Mater Continua 2021;66(1).
[2] Sultan K, Ikram M, Nguyen-Trong N. A multiband multibeam antenna for sub-6 GHz and mm-wave 5G applications. 21, (6):IEEE; 2022, p. 1278–82,
[3] Saeidi T, Alhawari AR, Almawgani AH, Alsuwian T, Imran MA, Abbasi Q. High gain compact UWB antenna for ground penetrating radar detection and soil inspection. Sensors 2022;22(14):5183.
[4] Saleem I, Rafique U, Agarwal S, SAVCI HŞ, Abbas SM, Mukhopadhyay S. Ultra-wideband fractal ring antenna for biomedical applications. Int J Antennas Propag 2023;2023.
[5] Saha TK, Knaus TN, Khosla A, Sekhar PK. A CPW-fed flexible UWB antenna for IoT applications. Microsyst Technol 2022;28(1):5–11.
[6] Li Z, Zhu X, Yin C. CPW-fed ultra-wideband slot antenna with broadband dual circular polarization. AEU-Int J Electron Commun 2019;98:191–8.
[7] Zhou X, Sun R, Zhao P, Cao Y, Yuan B, Chen S, et al. A novel design of a compact frequency-selective surface with high selectivity and angular stability. IEEE Microw Wirel Compon Lett 2022;32(7):931–4.
[8] Kundu S, Chatterjee A. A new compact ultra-wideband frequency selective surface with angular stability and polarization independence for antenna radiation enhancement in microwave imaging application. AEU-Int J Electron Commun 2022;155:154351.
[9] Tahir FA, Arshad T, Ullah S, Flint JA. A novel FSS for gain enhancement of printed antennas in UWB frequency spectrum. Microw Opt Technol Lett 2017;59(10):2698–704.
[10] Kundu S, Chatterjee A, Jana SK, Parui SK. A compact umbrella-shaped UWB antenna with gain augmentation using frequency selective surface. Radioengineering 2018;27(2):448–54.

[11] Fernandes EMF, da Silva MWB, da Silva Briggs L, de Siqueira Campos ALP, de Araújo HX, et al. 2.4–5.8 GHz dual-band patch antenna with FSS reflector for radiation parameters enhancement. AEU-Int J Electron Commun 2019;108:235–41.
[12] Saleem R, Bilal M, Shabbir T, Shafique MF. An FSS-employed UWB antenna system for high-gain portable devices. Microw Opt Technol Lett 2019;61(5):1404–10.
[13] Al-Gburi AJA, Ibrahim IBM, Zeain MY, Zakaria Z. Compact size and high gain of CPW-fed UWB strawberry artistic shaped printed monopole antennas using FSS single layer reflector. IEEE Access 2020;8:92697–707.
[14] Awan WA, Choi DM, Hussain N, Elfergani I, Park SG, Kim N. A frequency selective surface loaded UWB antenna for high gain applications. Comput, Mater Continua 2022;73(3).
[15] Din IU, Ullah S, Naqvi SI, Ullah R, Ullah S, Ali EM, et al. Improvement in the gain of UWB antenna for GPR applications by using frequency-selective surface. Int J Antennas Propag 2022;2022.
[16] Din IU, Ullah W, Abbasi NA, Ullah S, Shihzad W, Khan B, et al. A novel compact ultra-wideband frequency-selective surface-based antenna for gain enhancement applications. J Electromagn Eng Sci 2023;23(2):188–201.
[17] Hussain M, Sufian MA, Alzaidi MS, Naqvi SI, Hussain N, Elkamchouchi DH, et al. Bandwidth and gain enhancement of a CPW antenna using frequency selective surface for UWB applications. Micromachines 2023;14(3):591.
[18] Prasad N, Pardhasaradhi P, Madhav BTP, Islam T, Das S, El Ghzaoui M. Radiation performance improvement of a staircase shaped dual band printed antenna with a frequency selective surface (FSS) for wireless communication applications. Progr Electromagn Res C 2023;137:53–64.
[19] Tariq S, Hussain Q, Alzaidi MS, Ghoniem RM, Alibakhshikenari M, Althuwayb AA, et al. Frequency selective surfaces-based miniaturized wideband high-gain monopole antenna for UWB systems. AEU-Int J Electron Commun 2023;170:154841.
[20] Tahir MU, Rafique U, Ahmed MM, Abbas SM, Iqbal S, Wong S-W. High gain metasurface integrated millimeter-wave planar antenna. Int J Microw Wirel Technol 2023;1–12.